



Scientia Research Library

ISSN 2348-0424  
USA CODEN: JETRB4

Journal of Engineering And Technology Research,  
2014, 2 (5):47-56

<http://www.scientiaresearchlibrary.com/archive.php>

## Exact Solutions of Heat Transfer in Boundary Layer Flow over a Permeable Shrinking Sheet in the Presence of Radiation and Heat Source / Sink

Chandaneswar Midya

Department of Mathematics, Ghatal Rabindra Satabarsiki Mahavidyalaya, Paschim Medinipur,  
West Bengal - 721212, India

---

### ABSTRACT

An analytical study is presented to investigate the heat transfer characteristic of boundary layer flow over a linearly shrinking permeable sheet in the presence of radiation and heat source/sink. The governing boundary layer equations are reduced into ordinary differential equations by a similarity transformation. The reduced equations are then solved analytically for power-law surface temperature boundary conditions. The dual temperature is found to exist for any values of heat sink parameter for suction parameter  $s > 2$ . But in heat source case, the dual temperature may be obtained for  $s > 2$  subject to the condition  $\alpha > 2\sqrt{\lambda/DP_r}$ , where  $\lambda$  is the heat source/sink parameter,  $Pr$  the Prandtl number,  $D$  the parameter related to radiation and  $\alpha$  is the real positive root satisfying  $\alpha + 1/\alpha = s$ . But for physically valid flow and heat transfer real parameters, it difficult to satisfy the above condition for both the root  $\alpha$ . The effects of radiation parameter, Prandtl number, heat source/sink parameter, the wall mass transfer parameter on the temperature distribution are studied.

**Keywords:** Shrinking sheet, suction, boundary layer flow, Heat transfer, Thermal radiation, heat source/sink, Exact solution.

---

### INTRODUCTION

The boundary layer flow and heat transfer over a stretching surface is important in view of its application in several engineering processes. Since the pioneering work of Sakiadis [1,2], various aspects of the problem were investigated by many authors [3-12]. On the other hand, a little is known about the fluid flow and heat transfer over a shrinking sheet. In this type of flow, the fluid is shrunk towards a slot. In order to make the flow steady, some external force is needed to confine the vorticity inside the boundary layer. Suction at the sheet may sometimes play an important role in confining the vorticity inside the boundary layer. Wang [13] first proposed the flow over a shrinking sheet while working on the flow of a liquid film over an unsteady stretching sheet. Later, Miklavcic and Wang [14] obtained an analytical solution for steady viscous hydrodynamic flow over a permeable shrinking sheet. After that Hayat et al. [15] obtained the analytical solution of magneto-hydrodynamic flow of a second grade fluid over a shrinking sheet. Nadeem and Awais [16] studied thin film flow of an unsteady shrinking sheet through porous medium with variable

viscosity. Stagnation flow towards a shrinking sheet was studied by Wang [17]. Viscous flow over an unsteady shrinking sheet with mass transfer was studied by Fang and Zhang [18]. Ali et al. [19] studied magnetohydrodynamics viscous flow and heat transfer induced by a permeable shrinking sheet with prescribed surface heat flux. Sajid and Hayat [20] applied homotopy analysis method for the MHD viscous flow due to a shrinking sheet. Fang and Zhang [21] recently investigated the heat transfer characteristics of the shrinking sheet problem with a linear velocity. The effect of chemical reaction, heat and mass transfer on magnetohydrodynamic viscous flow due to a shrinking sheet in the presence of suction was studied by Muhaimin et al. [22]. Bhattacharyya [23] studied numerically the effects of heat source/sink on MHD flow and heat transfer over a shrinking sheet with mass suction. Numerical method cannot capture all the physics of shrinking sheet problem always. That is why there is a need to study these problems analytically. Midya [24] studied the magnetohydrodynamic viscous flow and heat transfer over a linearly shrinking permeable sheet without heat source/sink. Recently, Midya [25] obtained a closed form analytical solution for the distribution of heat in a MHD boundary layer flow over a non-permeable shrinking sheet with heat source/sink.

In this paper, the effect of thermal radiation on boundary layer heat transfer of the flow over a linearly shrinking permeable sheet in the presence of heat source/sink is investigated analytically for prescribed power-law wall temperature boundary condition. With the use of a similarity transformation the governing partial differential equations are reduced into ordinary differential equations which are then solved exactly. Temperature distributions are presented and discussed for various flow parameters.

## MATERIALS AND METHODS

### MATHEMATICAL FORMULATION

Let us consider a steady two-dimensional laminar flow of a viscous incompressible fluid over a continuously shrinking sheet. x-axis is chosen in the direction opposite the sheet motion and the y-axis is taken perpendicular to it. The shrinking sheet velocity is proportional to the distance i.e.  $u_w = -ax$ , ( $a > 0$ ) and the wall mass transfer velocity is  $v_w$ , with  $v_w > 0$  for injection and  $v_w < 0$  corresponds to suction.

The governing boundary layer equations for momentum and energy can be written as

$$\frac{\partial u}{\partial x} + \frac{\partial v}{\partial y} = 0 \quad (1)$$

$$u \frac{\partial u}{\partial x} + v \frac{\partial u}{\partial y} = \nu \frac{\partial^2 u}{\partial y^2} \quad (2)$$

$$u \frac{\partial T}{\partial x} + v \frac{\partial T}{\partial y} = \frac{\kappa}{\rho c_p} \frac{\partial^2 T}{\partial y^2} - \frac{1}{\rho c_p} \frac{\partial q_r}{\partial y} + \frac{Q}{\rho c_p} (T - T_\infty) \quad (3)$$

where  $u$  and  $v$  are the components of velocity respectively in the  $x$  and  $y$  directions,  $T$  is the temperature,  $\kappa$  is the thermal conductivity,  $c_p$  is the specific heat,  $\rho$  is the fluid density (assumed constant),  $\nu (= \mu/\rho)$  is the coefficient of fluid viscosity,  $q_r$  is the radiative heat flux,  $T_\infty$  is the temperature far from the sheet,  $Q$  is the volumetric rate of heat generation / absorption.

The boundary conditions for the velocity components and temperature are given by

$$u = -ax, \quad v = v_w, \quad T = T_w \quad \text{at } y = 0 \quad (4)$$

and

$$u \rightarrow 0, \quad v \rightarrow 0, \quad T \rightarrow T_\infty \quad \text{at } y \rightarrow \infty \quad (5)$$

where  $T_w$  is the wall temperature.

Now, Rosseland's approximation for radiation gives  $q_r = -\left(\frac{4\sigma}{3k_1}\right) \frac{\partial T^4}{\partial y}$ , where  $\sigma$  is the Stefan-Boltzmann constant,  $k_1$  is the Rosseland mean absorption coefficient (see Brewster [26]). It is assumed that the temperature variation within the flow is such that  $T^4$  may be expanded in a

Taylor's series. Expanding  $T^4$  about  $T_\infty$  and neglecting higher order terms, we have  $T^4 = 4T_\infty^3 T - 3T_\infty^4$ .

Therefore, Eq.(3) reduces to

$$u \frac{\partial T}{\partial x} + v \frac{\partial T}{\partial y} = \frac{\kappa}{\rho c_p} \frac{\partial^2 T}{\partial y^2} + \frac{16\sigma T_\infty^3}{3k_1 \rho c_p} \frac{\partial^2 T}{\partial y^2} + \frac{Q}{\rho c_p} (T - T_\infty) \quad (6)$$

## SOLUTION OF THE PROBLEM

Equations (1-2) along with the boundary conditions (4-5) admit self-similar solutions of the form

$$u = ax f'(\eta), \quad v = -\sqrt{av} f(\eta), \quad \eta = y \sqrt{\frac{a}{v}} \quad (7)$$

where  $f$  is the dimensionless stream function and  $\eta$  is the similarity variable. Substituting these, Eqs. (2) become

$$\frac{d^2 f}{d\eta^2} + f \frac{d^2 f}{d\eta^2} - \left(\frac{df}{d\eta}\right)^2 = 0 \quad (8)$$

The boundary conditions are

$$f'(0) = -1, \quad f(0) = s, \quad \text{and} \quad f'(\infty) = 0 \quad (9)$$

where  $s = -v_w / \sqrt{av}$  is a non-dimensional constant which determines the transpiration rate of the surface, with  $s > 0$  for suction and  $s < 0$  corresponds to injection.

There is an analytical solution (see Fang and Zhang [21]) for the equation with the boundary conditions given by

$$f(\eta) = \alpha + \frac{1}{\alpha} e^{-\alpha\eta}, \quad (10)$$

where  $\alpha = f(\infty) = f''(0)$  and  $\alpha (>0)$  can be obtained by solving the equation

$$\alpha + \frac{1}{\alpha} = s \quad (11)$$

It is, therefore, seen that there are two solutions for this equation for any  $s > 2$  and there is one solution for  $s = 2$ . No solution exists for  $s < 2$ . There is also an algebraically decaying solution as  $f(\eta) = \frac{s}{\eta + \sqrt{s}}$  for  $s = \sqrt{6}$ .

The non-dimensional horizontal velocity component is given by

$$f'(\eta) = -e^{-\alpha\eta} \quad (12)$$

The shear stress at the wall is denoted by  $\tau_w$  and is defined as

$$\tau_w = \mu (\partial u / \partial y)_{y=0} = \mu a x \sqrt{\frac{a}{v}} f''(0) = \mu a x \sqrt{\frac{a}{v}} \alpha \quad (13)$$

The skin friction coefficient  $C_f$  at the wall is obtained as

$$C_f = \frac{\tau_w}{(\mu a x \sqrt{\frac{a}{v}})} = f''(0) = \alpha \quad (14)$$

## HEAT TRANSFER ANALYSIS

First, we consider power-law surface temperature (PST) as surface boundary conditions and then power-law wall heat flux (PHF) case will be discussed.

### POWER-LAW SURFACE TEMPERATURE (PST) CASE

In this case the boundary conditions are

$$T = T_w = T_\infty + Ax^p \quad \text{at} \quad y = 0 \quad (15)$$

$$T \rightarrow T_\infty \quad \text{at} \quad y \rightarrow \infty \quad (16)$$

Defining the non-dimensional temperature  $\theta(\eta)$ , Prandtl number  $Pr$  and heat source / sink parameter  $\lambda$  as

$$\theta(\eta) = \frac{T - T_\infty}{T_w - T_\infty}, \quad Pr = \frac{\mu c_p}{\kappa}, \quad \lambda = \frac{Q}{\rho c_p a}$$

Using Eq. (7), we have from Eq. (6)

$$\frac{d^2 \theta}{d\eta^2} + DPr f \frac{d\theta}{d\eta} + DPr \left( \lambda - p \frac{df}{d\eta} \right) \theta = 0 \quad (17)$$

Here  $D=3R/(3R+4)$  and  $R$  is the thermal radiation parameter given by  $R=kk_1/4\sigma T_\infty^3$ .

The boundary conditions become

$$\theta(0) = 1, \text{ and } \theta(\infty) = 0. \quad (18)$$

Substituting the solution for the momentum transport the above Eq.(17) reduces to

$$\frac{d^2\theta}{d\eta^2} + DPr \left( \alpha + \frac{1}{\alpha} e^{-\alpha\eta} \right) \frac{d\theta}{d\eta} + DPr(\lambda + p e^{-\alpha\eta}) \theta = 0 \quad (19)$$

Now, let us introduce a new variable  $\xi = \frac{5\xi}{\alpha^2} e^{-\alpha\eta}$  so that the above equation transforms to

$$\xi \frac{d^2\theta}{d\xi^2} + (1 - DPr - \xi) \frac{d\theta}{d\xi} + \left( \frac{DPr\lambda}{\alpha^2\xi} + p \right) \theta = 0 \quad (20)$$

The boundary conditions (18) then become

$$\theta \left( \frac{DPr}{\alpha^2} \right) = 1, \text{ and } \theta(0) = 0 \quad (21)$$

Now, transforming the above equation (20) into confluent hypergeometric equation, we can obtain the solution (see Abramowitz and Stegun [27]) given by

$$\theta(\xi) = (\alpha^2\xi/DPr)^\beta \Phi(\beta - p, 1 + b_0, \xi) / \Phi(\beta - p, 1 + b_0, DPr/\alpha^2). \quad (22)$$

where  $\beta = (b_0 + a_0)/2$ ,  $a_0 = DPr$ ,  $b_0 = \sqrt{\alpha_0^2 - \frac{4\alpha_0\lambda}{\alpha^2}}$  and  $\Phi(a', b', x)$  is the confluent hypergeometric function of the first kind or Kummer function.

Now, in heat sink i.e. for negative values of  $\lambda$ ,  $b_0$  always becomes real because  $D$ ,  $Pr$  and  $\alpha$  are all positive. Therefore we should get two temperature profiles for all  $\lambda < 0$  corresponding to two exponential solutions for the momentum equation when  $s > 2$ . For  $s = 2$ , one temperature distribution can be obtained for any  $\lambda < 0$ .

In heat source case,  $\lambda$  becomes positive. Now  $b_0$  will have real value only when  $\alpha > 2\sqrt{\lambda/DPr}$ . Thus, in heat source case, dual temperature may be obtained for  $s > 2$  subject to the condition  $\alpha > 2\sqrt{\lambda/DPr}$ . But for physically valid flow and heat transfer real parameters, it difficult to satisfy the above condition for both the root  $\alpha$ . For  $s = 2$  and  $\alpha > 2\sqrt{\lambda/DPr}$ , only one temperature profile can be found in this case.

Therefore,

$$\theta(\eta) = e^{-\alpha\beta\eta} \Phi(\beta - p, 1 + b_0, DPr e^{-\alpha\eta}/\alpha^2) / \Phi(\beta - p, 1 + b_0, DPr/\alpha^2). \quad (23)$$

The dimensionless wall temperature gradient  $\theta'(0)$  is obtained as

$$\theta'(0) = -\alpha\beta - \frac{DPr}{\alpha} \frac{(\beta - p) \Phi(1 + \beta - p, 1 + b_0, DPr/\alpha^2)}{\Phi(\beta - p, 1 + b_0, DPr/\alpha^2)}. \quad (24)$$

## RESULTS AND DISCUSSION

Some examples showing temperature variations in the fluid are presented for certain values of the controlling parameters. For the mass suction parameter  $s = 3$ , we have two values of  $\alpha$  from Eq.(11) and they are  $\alpha = 2.618$  and  $0.382$ . We name  $\alpha = 2.618$  and  $\alpha = 0.382$  as first and second solution respectively. In all the following figures, the continuous lines represent the temperature distributions for first solution whereas second solution is represented by dotted one.

### Discussions for heat sink case

The dual temperature profiles for different values of the radiation parameter  $R$  ( $R = 0.5, 1.0, 1.5$ ) are depicted in Figure 1(a) for heat sink parameter  $\lambda = -0.3$ , power-index  $p = 2$  and suction parameter  $s = 3$ . It is seen that in case of the first solution, the temperature within the fluid is reduced throughout the boundary layer for increasing values of radiation parameter  $R$ . For the second solution, it is enhanced for increasing values of radiation parameter near the shrinking sheet. It is also observed that the boundary layer thickness for second solution is much higher than that of the first solution for fixed values of  $\eta$  near the shrinking sheet. At a large distance from the sheet the temperature takes its limiting value  $T_\infty$ .

Next, the temperature profiles for different values of the Prandtl number  $Pr$  ( $Pr = 0.5, 1.0, 1.5$ ) are depicted in Figure 1(b). The other parameters are  $R = 0.9$ ,  $s = 3$  ( $\alpha = 2.618, 0.318$ ),  $\lambda = -0.3$  and power index  $p = 1$ . It is seen that the increase of Prandtl number results in the decrease of temperature distribution. The increase of Prandtl number means slow rate of thermal diffusion. Because of reduced thermal conductivity, there would be a thinning of the thermal boundary layer and this leads to the decrease in the temperature.

The dual temperature profiles for different values of heat sink parameter  $\lambda$  ( $\lambda = -0.1, -0.3$  and  $-0.5$ ) are depicted in Figure 1(c). Here mass suction parameter  $s = 3$ ,  $Pr = 0.9$ ,  $R = 0.7$  and  $p = 1$ . The figure reveals that the temperature within the fluid decreases for the increasing values heat sink parameter  $\lambda$ . This fact is usual because of the fact that heat energy is absorbed in this case. Also it is to be noted that the boundary layer thickness for second solution is much higher than that of the first solution for fixed values of  $\eta$  near the shrinking sheet. The temperature overshoot at the wall is observed in the second solution for  $\lambda = -0.1$ .

Figure 1(d) represents the dual temperature distributions for various values the temperature power index  $p$  ( $p = 0, 1, 2$ ) with  $s = 3$ ,  $\lambda = -0.5$ ,  $R = 0.7$  and  $Pr = 0.9$ . It is noticed from the figure that the temperature within the fluid increases for the increasing values of power index  $p$  from 0 to 2 and this increase in temperature is very small for the first solution compared to the second solution.

We shall now concentrate on the temperature distribution for varying values of suction parameter  $s$  keeping other parameters fixed at  $R = 0.6$ ,  $Pr = 0.9$ ,  $\lambda = -0.2$  and power index  $p = 0$  and this is shown in Figure 1(e). We notice that the effect of suction parameter  $s$  is to decrease the temperature in the boundary layer for both the solutions.

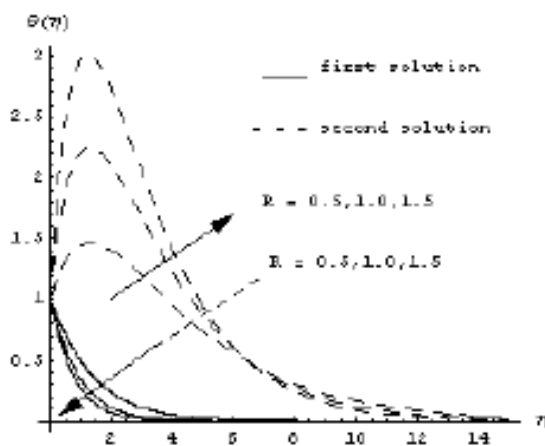


Figure 1(a) Variation of temperature for several values of  $R$  with  $s = 3$ ,  $Pr = 0.9$ ,  $\lambda = -0.3$  and  $p = 2$ .

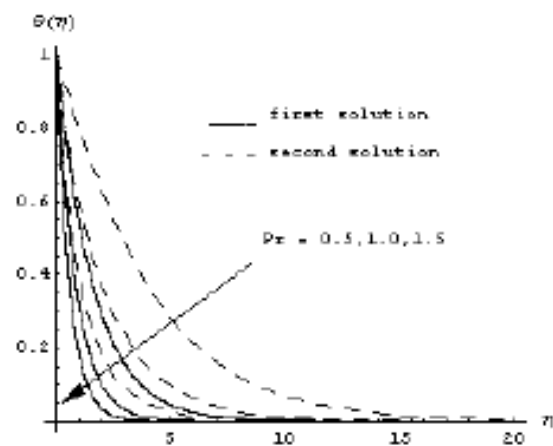


Figure 1(b) Dual temperature profiles for several values of  $Pr$  with  $s = 3$ ,  $R = 0.9$ ,  $\lambda = -0.3$  and  $p = 1$ .

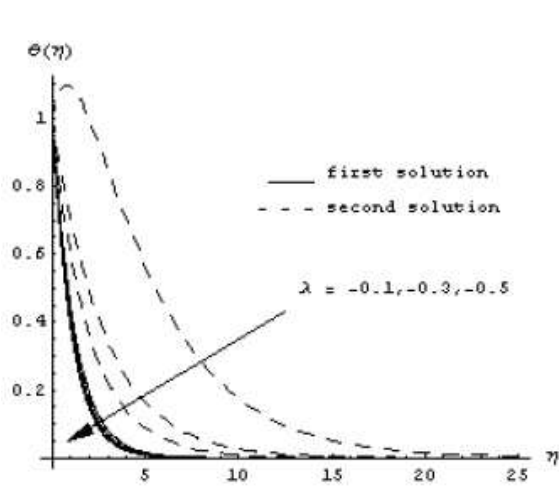


Figure 1(c) Variation of temperature for several values of  $\lambda$  with  $s = 3$ ,  $Pr = 0.9$ ,  $R = 0.7$  and  $p = 1$ .

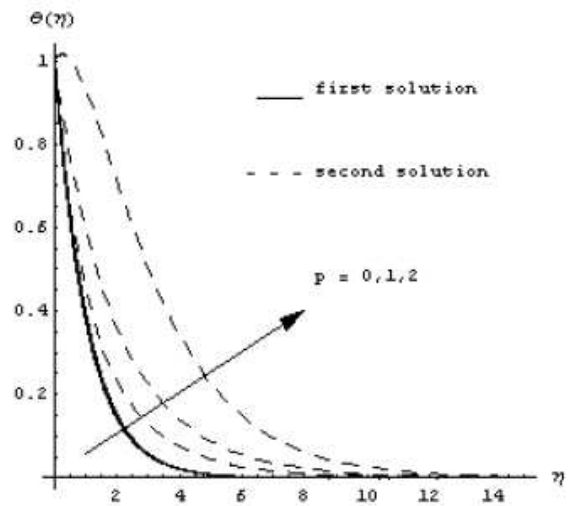


Figure 1(d) Dual temperature profiles for several values of  $p$  with  $s = 3$ ,  $Pr = 0.9$ ,  $\lambda = -0.5$  and  $R = 0.7$ .

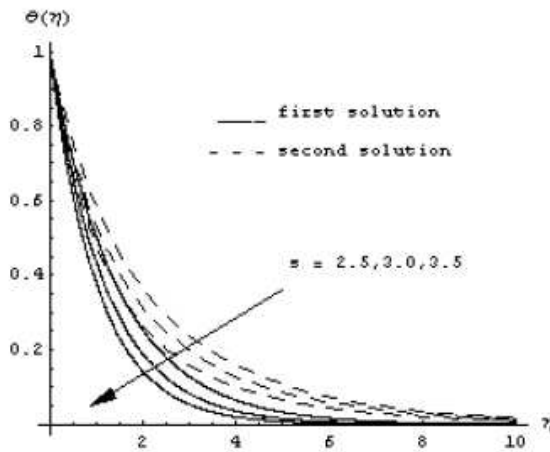


Figure 1(e) Dual temperature profiles for several values of  $s$  with  $R = 0.6$ ,  $Pr = 0.9$ ,  $\lambda = -0.2$  and  $p = 0$ .

**Discussions for heat source case**

Now we study the heat source case. We have already seen that in heat source case, dual temperature distribution corresponding to the two exponential solution exists for  $s > 2$  when  $\alpha > 2\sqrt{\lambda/DPr}$  is satisfied. Infact, for physically valid flow and heat transfer real parameters, it difficult to satisfy the above condition for both the root  $\alpha$ . When for  $s = 3$ , we have  $\alpha = 2.618$  and  $0.318$ . In the second solution the value of  $\alpha$  is small. Therefore, in this case, the condition  $\alpha > 2\sqrt{\lambda/DPr}$  is satisfied only when  $DPr$  is very large and heat source parameter is too small; otherwise the above condition will not be satisfied for the second solution. Thus, in heat source case, we study temperature distribution for first solution only.

First of all, the influence of radiation parameter  $R$  on the temperature profiles for first solution is presented in Figure 2(a) for  $Pr = 0.9$ ,  $s = 3$ ,  $\lambda = 0.3$  and  $p = 2$ . It is observed that increasing in radiation parameter  $R$  is to decrease temperature within the boundary layer. This can be explained by the fact that the increase of radiation parameter  $R$  implies the release of heat energy from the flow region by means of radiation and thereby temperature is decreased within the boundary layer

We shall now concentrate on the temperature distribution for first solution ( $\alpha = 2.618$ ) for different values of the Prandtl number  $Pr$  and it is shown in Figure 2(b). The other parameters are  $R = 0.9$ ,  $s = 3$ ,  $\lambda = 0.3$  and  $p = 1$ . It is seen that the increase of Prandtl number results in the decrease of temperature distribution throughout the boundary layer when heat source is present. Actually, the increase of Prandtl number means slow rate of thermal diffusion. Because of reduced thermal conductivity, there would be a thinning boundary layer and this leads to decrease in the temperature in the flow field.

The temperature profiles for first solution ( $\alpha = 2.618$ ) are depicted in Figure 2(c) for different values of the heat source parameters  $\lambda$  ( $\lambda = 0.1, 0.3, 0.5$ ). Here the radiation parameter is taken as  $R = 0.7$ ,  $s = 3$ ,  $pr = 0.9$  and  $p = 1$ . It is seen that the temperature within the fluid is increased if  $\lambda$  is increased. This is logical because internal heat energy emission results in an increase of heat transfer close to the shrinking sheet.

Now, we shall draw our attention to the effects of temperature distribution when the initial temperature is varied over the sheet. The temperature profiles for different values of power-law index  $p$  are plotted in Figure 2(d) for  $s = 3$ ,  $\lambda = 0.5$ ,  $Pr = 0.9$  and  $R = 0.7$ . It is observed from the figure that the temperature is increased very slowly with the increase of power-law index  $p$ .

Finally, the temperature profiles for various values of suction parameter  $s$  is presented in Figure 2(e) for fixed  $Pr = 0.9$ ,  $\lambda = 0.2$ ,  $R = 0.6$  and  $p = 0$  (in case of first solution  $\alpha = 2.618$ ). The figure reflects that the value of temperature at a particular  $\eta$  is reduced with increasing values of suction parameter  $s$ . Due to increase in the suction parameter  $s$ , the velocity boundary layer thickness becomes thinner and thinner and consequently decrease temperature within the fluid.

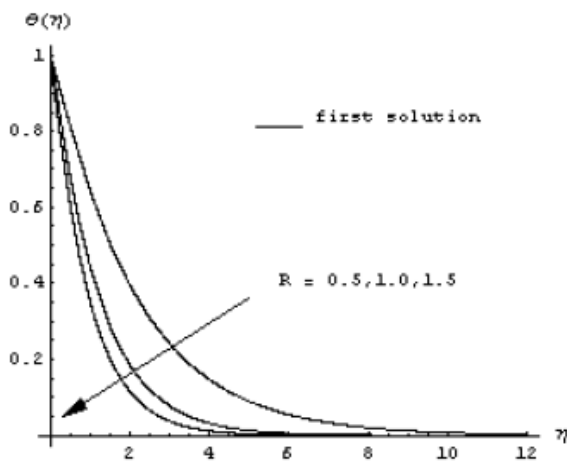


Figure 2(a) Variation of temperature for several values of  $R$  with  $s = 3$ ,  $Pr = 0.9$ ,  $\lambda = 0.3$  and  $p = 2$ .

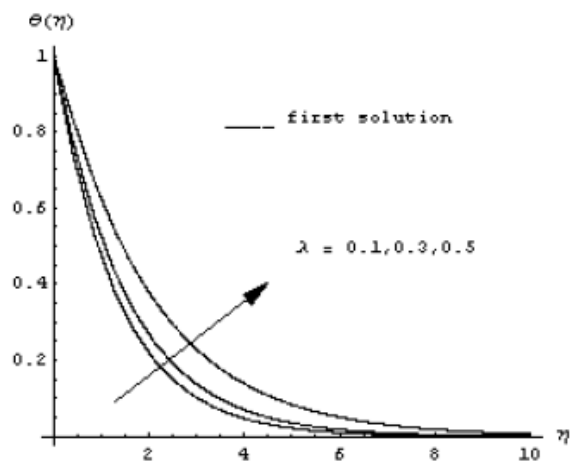


Figure 2(c) Variation of temperature for several values of  $\lambda$  with  $s = 3$  ( $\alpha = 2.618$ ),  $Pr = 0.9$ ,  $R = 0.7$  and  $p = 1$ .

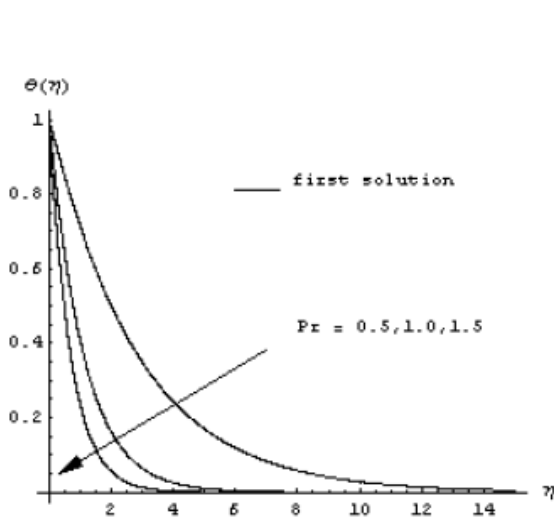


Figure 2(b) Temperature profiles for several values of Pr with  $s = 3$  ( $\alpha = 2.618$ ),  $R = 0.9$ ,  $\lambda = 0.3$  and  $p = 1$ .

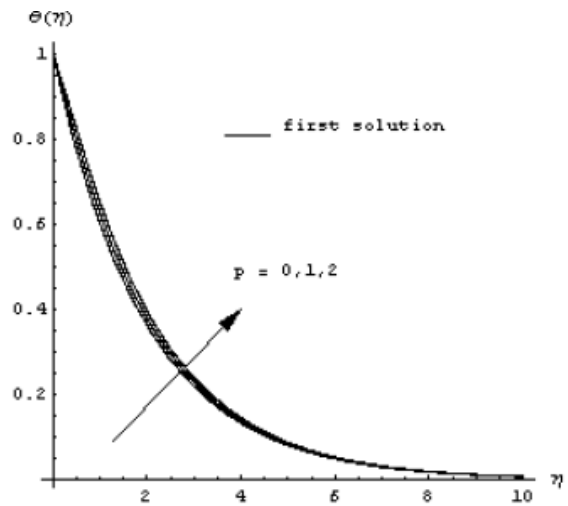


Figure 2(d) Temperature profiles for several values of p with  $s = 3$  ( $\alpha = 2.618$ ),  $Pr = 0.9$ ,  $\lambda = 0.5$  and  $R = 0.7$ .

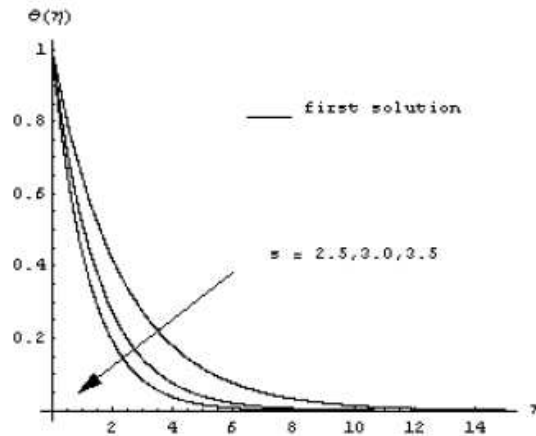


Figure 2(e) Variation of temperature for several values of s with  $R = 0.6$ ,  $Pr = 0.9$ ,  $\lambda = 0.2$  and  $p = 0$ .

### CONCLUSION

In conclusion, heat transfer over a linearly shrinking permeable surface with mass suction is investigated analytically in the presence of thermal radiation and heat source/sink. The exact analytical solutions of the boundary layer energy equation are obtained for power-law wall temperature boundary condition. The effects of radiation parameter  $R$ , Prandtl number  $Pr$ , heat source or sink parameter  $\lambda$ , the wall mass transfer parameter  $s$  and the power index  $p$  on the temperature distribution are studied. In heat sink case, dual temperature distribution is obtained for any  $s > 2$ , where  $s$  is the suction parameter. But in heat source case, dual temperature profiles may be obtained for  $s > 2$  with the condition  $\alpha > 2\sqrt{\lambda/DFr}$ . But, for physically valid flow and heat transfer real parameters, it difficult to satisfy the above condition for both the root  $\alpha$ . The temperature overshoot at the wall is observed for some cases.



## REFERENCES

- [1]. B. D. Sakiadis, Boundary-layer behavior on continuous solid surface:I.The Boundary-Layer equations for two-dimensional and asymmetric flow, *AIChE J*, 7, (1961), 26-28.
- [2]. B. C. Sakiadis, Boundary-layer behavior on continuous solid surface:II.The Boundary-Layer on a continuous flat surface, *AIChE J*, 7, (1961), 221-225.
- [3]. F. K. Tsou, E. M. Sparrow and R. J. Goldstain, Flow and heat transfer in the boundary layer on a continuous moving surface, *Int J Heat Mass Transfer*, 10, (1967), 219-235.
- [4]. L. J. Crane, Flow past a stretching plate, *Z Angew Math Phys*, 21, (1970), 645-647.
- [5]. P. S. Gupta, A. S. Gupta, Heat and mass transfer on a stretching sheet with suction and blowing, *Can J Chem Engng*, 77, (1977), 744-746.
- [6]. E. Magyari and B. Keller, Heat and mass transfer in the boundary layers on an exponentially stretching continuous surface, *J Phys D Appl Phys*, 32, (5), (1999), 577-585.
- [7]. K. R. Rajagopal, T. Y. Na and A. S. Gupta, Flow of a viscoelastic fluid over a stretching sheet, *Rhoel Acta*, 23, (1984), 213-215.
- [8]. H. S. Takhar, A. J. Chamkha and G. Nath, Flow and mass transfer on a stretching sheet with a magnetic field and chemically reactive species, *Int J Eng Sci*, 38, (2000), 1303-1314.
- [9]. Y. Y. Lok, N. Amin and I. Pop, Non-orthogonal stagnation point flow towards a stretching sheet, *Int J Non-Linear Mech*, 41, (2006), 622-627.
- [10]. S. J. Liao, A new branch solutions of boundary-layer flows over a permeable stretching plate, *Int J Nonlinear Mech*, 42, (2007), 819-830.
- [11]. E. M. A. Elbashbeshy, Heat transfer over a stretching surface with variable surface heat flux, *J Phys D Appl Phys*, 31, (1998), 1951-1954.
- [12]. M. E. M. Ouaf, Exact solution of thermal radiation on MHD flow over a stretching porous sheet, *Appl Math Comput*, 170, (2005), 1117-1125.
- [13]. C. Y. Wang, Liquid film on an unsteady stretching sheet, *Quart. Appl. Math.*, 48, (1990), 601-610.
- [14]. M. Miklavcic and C. Y. Wang, Viscous flow due to a shrinking sheet, *Quart Appl. Math.*, 64(2), (2006), 283-290.
- [15]. T. Hayat, Z. Abbas and M. Sajid, On the analytic solution of magnetohydrodynamic flow of a second grade fluid over a shrinking sheet, *J Appl Mech Trans ASME*, 74(6), (2007), 1165-1171.
- [16]. S. Nadeem and M. Awais, Thin film flow on an unsteady shrinking sheet through porous medium with variable viscosity, *Physics Letters A*, 372, (2008), 4965-4972.
- [17]. C. Y. Wang, Stagnation flow towards a shrinking sheet, *Int. J. Nonlinear Mech.*, 43, (2008), 377-382.
- [18]. T. Fang and J. Zhang, Viscous flow over an unsteady shrinking sheet with mass transfer, *Chin. Phys. Lett.*, 26(1), (2009), 014703-1-4.
- [19]. F. M. Ali, R. Nazar and N. M. Arifin, MHD viscous flow and heat transfer induced by a permeable shrinking sheet with prescribed surface heat flux, *WSEAS Trans on Math*, 9(5), (2010), 365-375.
- [20]. M. Sajid and T. Hayat, The application of homotopy analysis method for MHD viscous flow due to a shrinking sheet, *Chaos, Solitons and Fractals*, 39(3), (2009), 1317-1323.
- [21]. T. Fang and J. Zhang, Thermal boundary layer over a shrinking sheet : an analytical solution, *Acta Mech*, 209, (2010), 325-343.
- [22]. Muhaimin, R. Kandasamy, I. Hashim and A. B. Khamis, On the effect of chemical reaction, heat and mass transfer on nonlinear MHD boundary layer past a porous shrinking sheet with suction, *Theoretical and Applied Mechanics*, 36(2), (2009), 101-116.
- [23]. K. Bhattacharyya, Effects of heat source/sink on MHD flow and heat transfer over a shrinking sheet with mass suction, *Chem. Engg. Res. Bulletin* 15 (2011) 12-17.

- [24]. C. Midya, Hydromagnetic boundary layer flow and heat transfer over a linearly shrinking permeable surface, *Int. J. Appl. Math. Mech.*, 8(3), (2012), 57-68.
- [25]. C. Midya, Heat transfer in MHD boundary layer flow over a shrinking sheet with radiation and heat sink, *J. G. Res. In Math. Archive*, 1(2), (2013), 63-70.
- [26]. M. Q. Brewster, *Thermal Radiative Transfer Properties*, John Wiley and Sons, (1972).
- [27]. M. Abramowitz, I. A. Stegun, *Handbook of Mathematical Functions*, Dover Publications, New York, (1972).